Altered Na^+ transport after an intracellular α-subunit deletion reveals strict external sequential release of Na^+ from the Na/K pump

Siddhartha Yaragatupalli[a], J. Fernando Olivera[a], Craig Gatto[b], and Pablo Artigas[a,1]

[a]Department of Cell Physiology and Molecular Biophysics, Texas Tech University Health Sciences Center, Lubbock, TX 79430; and [b]School of Biological Sciences, Illinois State University, Normal, IL 61790-4120

Edited by Francisco Bezanilla, The University of Chicago, Chicago, IL, and approved July 22, 2009 (received for review April 6, 2009)

The Na/K pump actively exports 3 Na^+ in exchange for 2 K^+ across the plasmalemma of animal cells. As in other P-type ATPases, pump function is more effective when the relative affinity for transported ions is altered as the ion binding sites alternate between opposite sides of the membrane. Deletion of the five C-terminal residues from the α-subunit diminishes internal Na^+ (Na_i^+) affinity ≈25-fold [Morth et al. (2007) *Nature* 450:1043–1049]. Because external Na^+ (Na_o^+) binding is voltage-dependent, we studied the reactions involving this process by using two-electrode and inside-out patch voltage clamp in normal and truncated (ΔKESYY) Xenopus-α1 pumps expressed in oocytes. We observed that ΔKESYY (*i*) decreased both Na_o^+ and Na_i^+ apparent affinities in the absence of K_o^+, and (*ii*) did not affect apparent Na_o^+ affinity at high K_o^+. These results support a model of strict sequential external release of Na^+ ions, where the Na^+-exclusive site releases Na^+ before the sites shared with K^+ and the ΔKESYY deletion only reduces Na_o^+ affinity at the shared sites. Moreover, at nonsaturating K_o^+, ΔKESYY induced an inward flow of Na^+ through Na/K pumps at negative potentials. Guanidinium$^+$ can also permeate truncated pumps, whereas N-methyl-D-glucamine cannot. Because guanidinium$_o^+$ can also traverse normal Na/K pumps in the absence of both Na_o^+ and K_o^+ and can also inhibit Na/K pump currents in a Na^+-like voltage-dependent manner, we conclude that the normal pathway transited by the first externally released Na^+ is large enough to accommodate guanidinium$^+$.

C-terminal truncation | ion access channel | ion binding | Na,K-ATPase | voltage dependence

The essential electrochemical gradient for Na^+ ions across the plasma membrane of most animal cells is maintained by the Na/K pump, a heterodimeric P-type ATPase, which like other P-type 2C ATPases is composed of a catalytic α subunit and a β subunit (essential for membrane trafficking). The reaction cycle of the Na/K pump (like most P-type ATPases) is described by a set of reversible partial reactions known as the Post-Albers scheme (1, 2), shown superimposed with a cartoon representation of the pump's ion-binding and ion-unbinding reactions in Fig. 1. The high-resolution structure of the Na/K pump in the $E2(K_2^+)$MgF transition state (3) reveals the relative position and interaction between the α, β, and γ subunits (γ is a regulatory subunit present in several tissues) (4), and the coordination of K^+ ions within the α-subunit's transmembrane segments. Coordination of two of the three Na^+ ions is similar to that of the two countertransported K^+ ions (represented by the center and right-hand sites in Fig. 1), but the other Na^+ ion binds to a Na^+-exclusive site (left-hand site in Fig. 1) (5, 6).

Extrusion of one net charge per cycle because of the $3Na^+/2K^+$ stoichiometry makes the Na/K pump an electrogenic voltage-dependent transporter. The more voltage-sensitive partial reactions are those reactions involving ion binding and release through a channel-like structure accessible from the extracellular space (Fig. 1) (7–10). Because the Na^+-transport branch is more voltage-sensitive (8, 11) than the K^+-transport branch (7, 12), under physiological conditions with high Na_o^+, negative transmembrane voltages inhibit the pump by forcing Na^+ ions back into the access channel producing a steep positive slope in the steady-state Na/K pump current (I_P) versus V curve. Thus, the position of the I_P–V curve on the voltage axis depends on the $[Na_o^+]$ and the apparent Na_o^+ affinity. Mutations that affect Na_o^+ binding have been shown to induce parallel shifts in this curve across the voltage axis (6), similar to those produced by changing $[Na_o^+]$ in normal pumps (9, 13).

In the absence of K_o^+, but presence of Na_o^+, the pump shuttles between Na^+-bound and unbound states in a voltage-dependent manner. Step changes in membrane potential elicit transient currents known as Na^+-dependent transient charge movement (14), which follow a multiexponential time course related to the sequential release of three Na^+ ions (11, 15). With positive voltage pulses, the slowest exponential term, believed to represent diffusion-limited release of the first Na^+ through a narrow access channel of unknown structure (as schematized in Fig. 1), is rate limited by the electroneutral E1-E2 transition. However, with negative pulses, transient currents are rate-limited by binding of the ions to their binding sites deep inside an access channel whose occupancy is controlled by voltage and $[Na_o^+]$. The voltage dependence of the total charge moved in the slow component (Q_{tot}) follows a Boltzmann distribution centered at a voltage ($V_{1/2}$) in which half the pumps are in E2 and half are in E1. Thus, analogous to the parallel shifts in the I_P–V curve, the center of this so-called Q–V curve depends on $[Na_o^+]$ (11, 16).

The Na/K pump's efficacy to transport ions depends on the change in affinity of the ion binding sites from high affinity for Na^+ ($K_{0.5,Na} \leq 1$ mM; $K_{0.5,K} \approx 10$ mM in the presence of ATP, depending on $[Mg^{2+}]$) (17) when facing internally (E1 states, bottom row in Fig. 1) to high affinity for K^+ ($K_{0.5,K} \leq 0.2$ mM; $K_{0.5,Na} \approx 100$ mM, depending on voltage) when externally exposed in E2 (E2P states, top row in Fig. 1) (18). Morth et al. (3) reported a ≈25-fold reduction in Na_i^+ affinity by deletion of the last five C-terminal residues of the α-subunit (ΔKETYY; pig α1-subunit). That finding prompted us to examine the effects of this deletion on Na_o^+ affinity by analyzing voltage-dependent reactions. We observed a reduction in Na_o^+ affinity that was only apparent on the Q–V curve, but not on the I_P–V curve. In addition, we found that the C-terminal deletion induces the appearance of an inward Na^+ current through the Na/K pump and that guanidinium$^+$ ions can not only traverse mutant pumps, but can also inhibit normal Na/K pumps in a voltage-dependent manner. These observations provide insight into understanding

Author contributions: P.A. designed research; S.Y., J.F.O., C.G., and P.A. performed research; P.A. analyzed data; and C.G. and P.A. wrote the paper.

The authors declare no conflict of interest.

This article is a PNAS Direct Submission.

[1]To whom correspondence should be addressed. E-mail: pablo.artigas@ttuhsc.edu.

This article contains supporting information online at www.pnas.org/cgi/content/full/0903752106/DCSupplemental.

PHYSIOLOGY

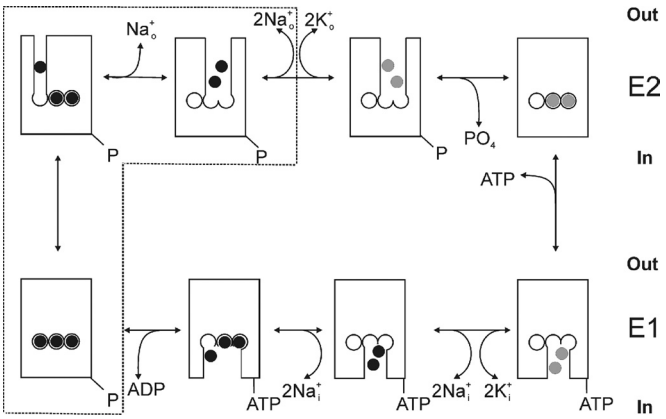

Fig. 1. Albers-Post kinetic scheme of the Na/K pump shown superimposed with a cartoon representation of transitions involving binding and release of ions. Na^+ ions (black), K^+ ions (gray). The box encloses states involved in Na^+-dependent charge movement.

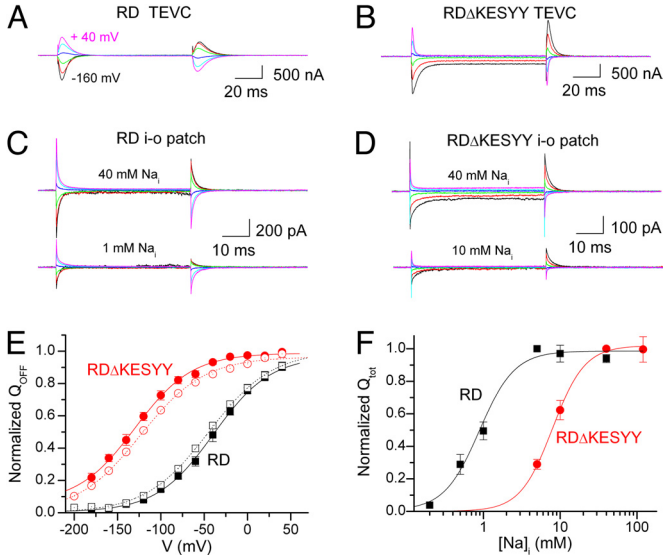

Fig. 2. Transient charge movement in the presence of Na_o^+ and absence of K_o^+. (*A* and *B*) Ouabain-sensitive (10 mM) currents were measured in 125 mM Na^+ solution via TEVC from Na^+-loaded oocytes injected with RD-α1 cRNA (*A*) and RDΔKESYY-α1 cRNA (*B*) two days postinjection. Currents elicited by 100-ms pulses from $V_h = -50$ mV to voltages ranging from -160 mV to $+40$ mV in 40-mV increments. Endogenous pumps were inhibited by preincubation with 10 μM ouabain (see *Methods*). The speed of the clamp was slower ($\tau = 340$ μs) for the experiment in *A* than for that in *B* ($\tau = 150$ μs). (*C* and *D*) Na_i^+-induced currents were measured in giant inside-out patches. All measurements were performed in presence of 4 mM MgATP at 4–6 days postinjection with either RD-α1 cRNA (*C*) or RDΔKESYY-α1 cRNA (*D*). The 125 mM Na_o^+ (intrapipette) solution contained 1 μM ouabain to inhibit endogenous pumps. Traces are the difference between currents observed in the absence and presence of the indicated $[Na_i^+]$. (*E*) Voltage dependence of normalized Q_{OFF} from ouabain-sensitive currents in TEVC or 40 mM Na_i^+-induced currents in patches. Data from whole oocytes injected with RD (n = 6) (black open squares) or RDΔKESYY (n = 8) (red open circles) were fitted to a Boltzmann distribution (dotted lines). RD parameters were: $V_{1/2} = -39$ mV, $k_B = 33$ mV, with a $Q_{tot} = 8.6 \pm 1.7$ nC and $I_{3K,NMG} = 135 \pm 24$ nA (i.e., current activated by 3 mM K in NMG). RDΔKESYY parameters were: $V_{1/2} = -130$ mV, $k_B = 33$ mV, with a $Q_{tot} = 14.8 \pm 2.6$ nC and $I_{3K,NMG} = 195 \pm 30$ nA. Data from inside-out patches from oocytes expressing RD (black filled squares; n = 8) or RDΔKESYY (red filled circles; n = 7) pumps were also fitted to Boltzmann distribution (solid lines). RD parameters were: $V_{1/2} = -41$ mV, $k_B = 32$ mV, with a $Q_{tot} = 491 \pm 136$ fC. RDΔKESYY parameters were: $V_{1/2} = -135$ mV and $k_B = 33 \pm 2$ mV, with a $Q_{tot} = 442 \pm 70$ fC. (*F*) Q_{tot} was calculated from the Boltzmann fit to the Q–V curves at different Na_i^+, normalized to the value at 5 mM Na_i^+ (RD), or 40 mM (RDΔKESYY), and plotted as a function of $[Na_i^+]$. Data were fitted to the Hill equation with parameters in *Results*.

the sequential nature of external release of Na^+ ions in the Na/K pump.

Results

Heterologous expression and delivery of the full-length ouabain-resistant ($IC_{50} \approx 200$ μM) mutant of the Xenopus α1 subunit, RD (see *Methods*), and its C-terminal truncated form, RDΔKESYY, to the plasma membrane of Xenopus oocytes was confirmed via Western blot analysis of isolated plasma membrane proteins (Fig. S1).

Effects on Na_o^+- and Voltage-Dependent Reactions. Voltage dependence of transient charge movement was examined in the absence of K_o^+ (Fig. 2). Oocytes were Na^+-loaded in the presence of ouabain to inhibit endogenous Na/K pumps (see *Methods*) and then studied under two-electrode voltage clamp (TEVC) with an external solution containing 125 mM Na^+. Pump-related (i.e., difference between presence and absence of 10 mM ouabain) transient signals elicited from a holding potential (V_h) of -50 mV by 100 ms-long step pulses from -200 mV to $+60$ mV (20-mV increments) were measured. Fig. 2 *A* and *B* illustrate ouabain-sensitive currents in oocytes expressing the control RD and the RDΔKESYY deletion mutant, respectively (only every other trace from -160 mV is shown). The KESYY deletion has three effects: first, an increased inward steady-state current at negative potentials; second, loss of transient currents moved by positive pulses; and third, a reduced voltage-dependent increase in the rate of charge movement at negative potentials.

We also measured transient charge movement by the Na/K pump in giant inside-out patches. Because these currents require pump phosphorylation, the signals were MgATP and Na_i^+-dependent. At 125 mM Na_o^+ (intrapipette), Na_i^+-dependent currents (currents in the presence of Na_i^+ minus currents in absence of Na_i^+) were measured at 4 mM MgATP in inside-out giant patches from oocytes expressing RD control (Fig. 2*C*) or RDΔKESYY mutants (Fig. 2*D*). [ATP]-dependence could not be studied because of nucleotide-dependent patch instability at the negative potentials required to study RDΔKESYY. The top traces depict currents elicited by pulses to the same voltages as in Fig. 2 *A* and *B*, but induced by application of 40 mM Na_i^+, whereas the bottom traces were induced by either 1 mM (RD) or 10 mM Na_i^+ (RDΔKESY) in the same patches.

Ouabain-sensitive currents in whole oocytes under TEVC and 40 mM Na_i^+-induced currents in patches were fitted with a single exponential, omitting the first 3 ms in TEVC (to avoid clamp artifacts) or the first 300 μs for patches (to exclude the fast component). The charge at the beginning (Q_{ON}) and end (Q_{OFF}) of the pulse was estimated by integration over time of the exponential fits. Q_{ON} and Q_{OFF} were identical in patch experiments, but Q_{ON} was larger ($\approx$10%) than Q_{OFF} in TEVC, likely because of clamp limitations. Hence, we compared the equilibrium distribution of normalized Q_{OFF} (Fig. 2*E*) in RD (black symbols) and RDΔKESYY (red symbols) measured with both TEVC (open symbols) and patches (filled symbols). A remarkable observation with both techniques is that the RDΔKESYY mutation induced a pronounced shift ≈ -100 mV in the charge distribution, which suggests a reduction in apparent Na_o^+ affinity.

The $[Na_i^+]$ dependence of total Q_{OFF} (Q_{tot}) was also examined, revealing the expected reduction in Na_i^+ affinity for RDΔKESYY (Fig. 2*F*). The best fit of the Hill equation to the average data gave $K_{0.5Na} = 0.8 \pm 0.1$ mM ($n_H = 2.5 \pm 0.6$) and 9 ± 1 mM ($n_H = 1.8 \pm 0.4$) for the RD (n = 5) and RDΔKESYY (n = 6), respectively. Therefore, the C-terminal deletion reduces Na^+ affinity on both sides of the membrane.

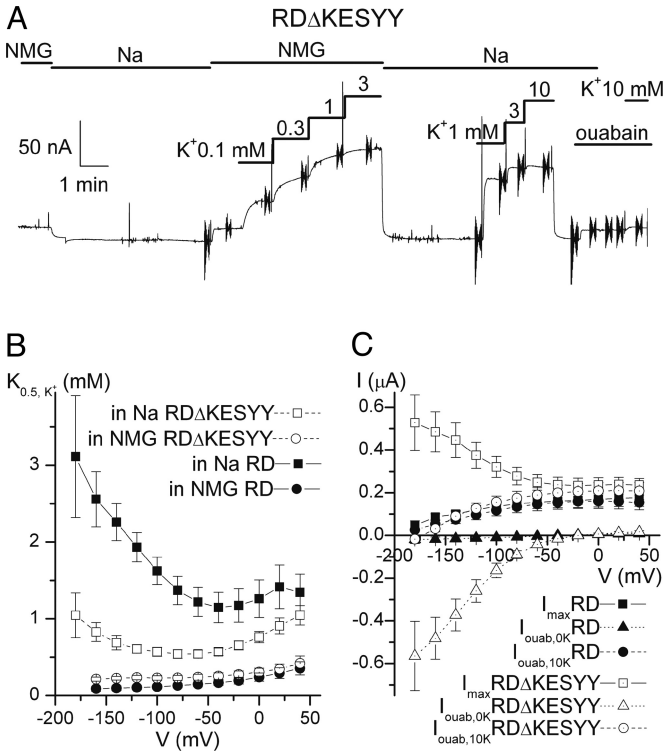

Fig. 3. Steady-state Na/K pump-related currents. (*A*) Continuous TEVC trace from a Na^+-loaded oocyte (V_h = −50 mV, 3 days postinjection) expressing RDΔKESYY. Increasing $[K^+_o]$ induced an outward current, both in the presence and absence of 125 mM Na^+_o (replaced with 125 mM NMG^+_o). Vertical deflections correspond to 50-ms square voltage pulses, where the average current during the last 5 ms was measured. K^+_o-induced currents (i.e., difference between K^+_o and no K^+_o) at each voltage were plotted as a function of $[K^+_o]$ and fitted with a Hill equation to obtain $K_{0.5app}$ values. (*B*) $K_{0.5}$ vs. voltage curves from RD injected oocytes in NMG^+_o (filled circles) and Na^+_o (filled squares), and from RDΔKESYY injected ooctyes in NMG^+_o (open circles) and Na^+_o (open squares). The Hill coefficients for the fits were: RD $n_H = 1.2 \pm 0.2$ in NMG^+_o, $n_H = 1.4 \pm 0.1$ in Na^+_o; RDΔKESYY, $n_H = 1.2 \pm 0.04$ in NMG^+_o, $n_H = 1.5 \pm 0.1$ in Na^+_o. (*C*) Current-voltage relationships measured in 125 mM Na^+_o. Normalized maximum K^+_o-induced current from Hill fits (I_{max}, squares), together with ouabain-sensitive currents at 10 mM K^+_o ($I_{ouab,10K}$, circles) and 0 mM K^+_o ($I_{ouab,0K}$, triangles) are shown from oocytes injected with RD (filled symbols) and RDΔKESYY pumps (open symbols). In all cases endogenous pumps were inhibited by application of 10 μM ouabain in the Na^+-loading solution (see *Methods*).

The voltage sensitivity of pump-related steady-state currents was studied in Na^+-loaded oocytes under TEVC (Fig. 3) in the presence and absence of Na^+_o (replacing Na^+_o with N-methyl-D-glucamine^+_o (NMG^+_o) to avoid competition between transported ions). A continuous TEVC current recording from an oocyte expressing RDΔKESYY held at −50 mV shows that stepwise increments in $[K^+_o]$ induced outward current deflections in a saturating fashion (Fig. 3*A*). Steep vertical deflections in the continuous trace correspond to 50-ms square pulses applied from −180 to +40 mV to study voltage dependence of steady state current. The K^+_o-induced currents (average of the last 5 ms) were plotted against $[K^+_o]$ and fitted with the Hill equation. Fig. 3*B* shows the $K_{0.5}$ from those fits as a function of voltage for the RD control (filled symbols) and for the RDΔKESYY (open symbols), in the presence (squares) and absence of Na^+_o (circles). The RDΔKESYY deletion induced a clear increase in apparent affinity for K^+_o (reduction of its $K_{0.5}$), which is only observed in the presence of Na^+_o, also consistent with a reduction in apparent affinity for Na^+_o (which competes with K^+_o for occupation of the pump in a ping-pong mechanism).

We investigated further the voltage dependence of steady-state pump currents at 125 mM Na^+_o (Fig. 3*C*). Control RD pumps present a positive slope both in the I_{max}–V curve (filled squares, obtained from the Hill fits) and in the ouabain-sensitive current in 10 mM K^+_o (filled circles), which display almost identical voltage dependencies (curves at lower $[K^+_o]$ are shifted to the right) (13). However, similar analyses of voltage effects in oocytes expressing RDΔKESYY are complicated by a large inward current observed at 0 mM K^+_o (open triangles, Fig. 3*C*), which is not seen in RD pumps (filled triangles). Thus, the outward current induced by K^+_o binding to its transport sites in RDΔKESYY pumps represents two phenomena: (*i*) the induction of normal I_P (i.e., stoichiometric $3Na^+/2K^+$ transport) and (*ii*) the inhibition of the inward current at negative potentials. (Note that maximal K^+-induced current and current inhibited by ouabain in 10 mM K^+ are identical at voltages where there is no inward current in the absence of K^+_o, indicating that K^+-induced currents are indeed pump-related.) This inward current is responsible for the negative slope in the I_{max}–V curve (open squares); a similar negative slope is observed in control pumps in the absence of Na^+_o (Fig. S2). Because the inward current is inhibited both by 10 mM K^+_o and by ouabain, practically all of the ouabain-sensitive current with 10 mM K^+_o (open circles) corresponds to I_P. The curves from RD and RDΔKESYY pumps fall on top of each other, indicating that the inward current masked the normal voltage dependence of I_P in truncated pumps.

Characteristics of the Inward Current. The Na^+_o-dependent inward current observed in the RDΔKESYY (at low $[K^+_o]$ and negative potentials) was accompanied by the disappearance of a H^+ current (of smaller amplitude at pH 7.6) observed in RD pumps in the absence of Na^+_o and K^+_o (Fig. S2). This H^+ current has been described in endogenous (12), wild-type (19), and mutant Na/K pumps (20, 21) expressed in Xenopus oocytes and has been proposed to represent downhill transport of H^+ through the exclusive Na^+ binding site when the pump is in E2P (21, 22). As the two currents present similar voltage dependencies, TEVC was used to study the $[Na^+_o]$ dependence of ouabain-sensitive steady-state current in the absence of K^+_o in RDΔKESYY pumps. The inward current increased linearly with $[Na^+_o]$ up to 125 mM (Fig. S3) consistent with a low affinity Na^+ passive flow through ΔKESYY pumps.

Guanidinium$^+$ (gua^+) ions compete with Na^+_i for binding to the Na/K pump (23) and have been shown to permeate voltage-dependent Na^+ channels [VNaC (24), but not epithelial Na^+ channels (25)]. To test whether gua^+ is a Na^+-surrogate and can sustain inward currents through truncated pumps, we measured ouabain-sensitive currents with 120 mM gua^+_o (Fig. 4*A Top*). At −180 mV the steady-state inward current in gua^+_o was ≈10-fold larger than those in 120 mM Na^+_o measured in the same oocyte (Fig. 4*A Bottom*). The time course of current increase at potentials negative to −140 mV was described with a double exponential fit with a poorly resolved fast component ($\tau_{fast} \approx 3$ ms) and a slow component that became more prominent (Fig. 4*B*, filled circles) and slower (Fig. 4*B*, open circles) at more negative voltages.

As it seems plausible that the Na^+_o-dependent inward currents in RDΔKESYY and the H^+-leak in RD control pumps are related phenomena, we studied ouabain-sensitive currents in RD-expressing oocytes bathed with 120 mM gua^+_o (Fig. 4*C Top*) or 120 mM Na^+_o (Fig. 4*C Bottom*, same oocyte as in *Top*). The large inward current observed with 120 mM gua^+_o, which follows a fast single-exponential time course ($\tau = 4.8 \pm 0.9$ ms, n = 6 at −180 mv), was reduced by 53 ± 2% (n = 5) when the $[gua^+_o]$ was cut in half (replacing with NMG^+_o), consistent with gua^+ ions being the charge carrier. The maximal amplitude of the ouabain-sensitive current in 120 mM gua^+ as a function of voltage for the RD (filled squares) and the RDΔKESYY mutant (open circles, estimated from biexponential fits) is shown in Fig. 4*D* (normal-

PHYSIOLOGY

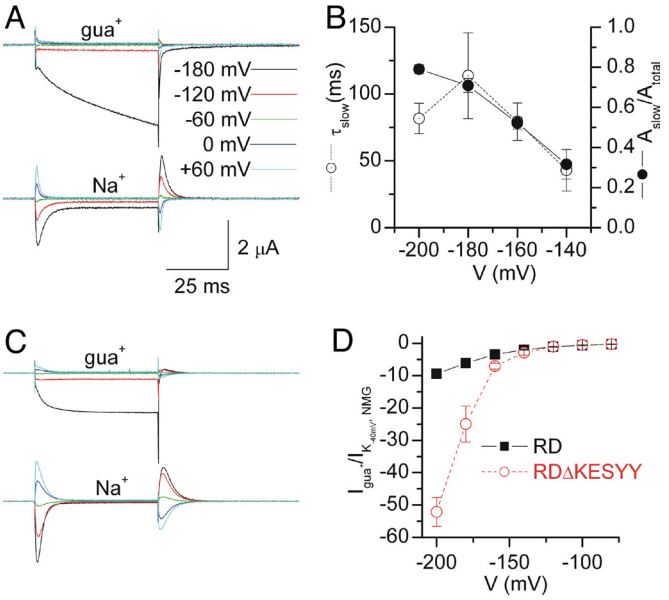

Fig. 4. Ouabain-sensitive guanidinium$^+$-dependent currents. (*A*) Ouabain-sensitive currents elicited by indicated voltage pulses, from $V_h = -50$ mV. TEVC traces are from an oocyte injected with RDΔKESYY in 120 mM gua^+_o (*Upper*) or 120 mM Na^+_o (*Lower*). (*B*) Voltage dependence of the relative amplitude (filled circles) and τ (open circles) of the slow component from biexponential fits to the traces in 120 mM gua^+_o. (*C*) Same as in *A* but from an RD-injected oocyte. (*D*) Steady-state current (normalized to the 3 mM K^+_o-induced current at −50 mV in NMG^+_o) measured from RD (filled black squares) and RDΔKESYY (open red circles, estimated from biexponential fits) expressing oocytes in 120 mM gua^+_o.

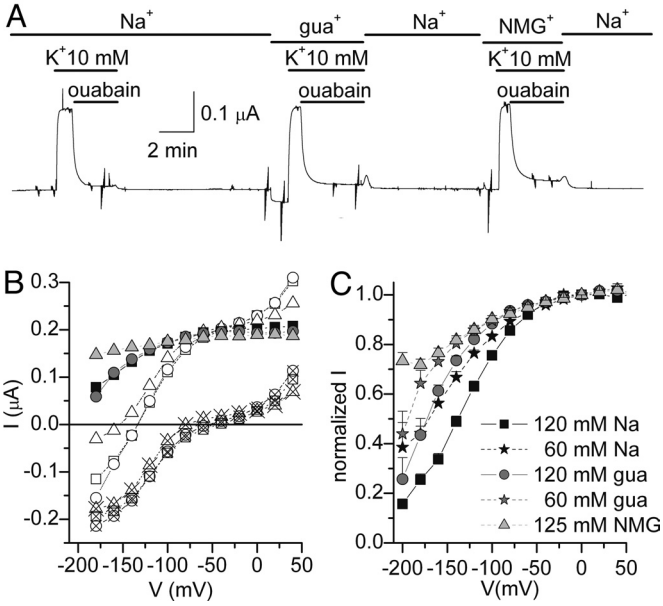

Fig. 5. Voltage-dependent inhibition of Na/K pump current by guanidinium^+_o in RD pumps. (*A*) Continuous TEVC trace from a Na^+-loaded oocyte at $V_h = -50$ mV. K^+_o-induced outward currents and ouabain inhibited Na/K pump current. To prevent Na^+_i depletion because of diffusion, the long recovery following pump inhibition was made in Na^+_o solution. (*B*) Steady-state I–V relationships obtained in 10 mM K^+_o, in the absence (open symbols) or presence (open crossed symbols) of 10 mM ouabain with either 120 mM Na^+_o solution (squares), 120 mM gua^+_o solution (circles), or 125 mM NMG^+_o (triangles). The ouabain-sensitive currents are presented as filled symbols. (*C*) I_P (ouabain-sensitive currents in 10 mM K^+_o) vs. voltage plot, normalized to the current observed at 0 mV with five different external ionic conditions: 120 mM Na^+_o (black squares), 120 mM gua^+_o (gray circles), 60 mM Na^+_o (black stars), 60 mM gua^+_o (gray stars), and 125 mM NMG (light gray triangles).

ized to current activated by 3 mM K^+_o in NMG^+_o at −40 mV to correct for expression levels). The two curves deviate from each other at the negative voltages, where an increase of the relative amplitude of the slow component in RDΔKESYY expressing oocytes was observed (Fig. 4 *B* and *D*). This observation may indicate that the fast component (with similar absolute amplitude in RD and RDΔKESYY) represents gua^+ permeation across the Na^+-only binding site in both pumps (experiments characterizing the slow component are underway, but beyond the scope of this report).

To date, no organic ion has been shown to inhibit pump currents in a "Na^+_o-like" voltage-dependent manner. Thus, if gua^+ enters the access channel to the Na^+-exclusive site, and we know that Na^+_o rebinding to this site is the main cause for the positive slope in the I_P–V curves (as in Fig. 3), then one may expect to observe voltage-dependent inhibition of I_P in the presence of high gua^+_o in RD pumps at near-saturating K^+_o. Fig. 5*A* shows the continuous TEVC recording from an oocyte held at −50 mV, where 10 mM K^+_o-induced currents were subsequently inhibited by ouabain in the presence of either 120 mM Na^+_o, 120 mM gua^+_o, or 125 mM NMG^+_o. Fig. 5*B* displays the steady-state I–V relationships in the absence (open symbols) and presence of ouabain (× symbols) in the three cation solutions, together with the ouabain-sensitive current (I_P, filled symbols) obtained by subtraction of those curves. Clearly, the I_P voltage-sensitivity is similar in gua^+_o (gray circles) and Na^+_o (black squares), but different from NMG^+_o (dotted triangle). The voltage-dependence of I_P at different concentrations of the main cations is consistent with a lower affinity for gua^+_o than Na^+_o, given that the curve observed in 120 mM gua^+_o (gray circles, n = 16) nearly overlaps with 60 mM Na^+_o (black stars, n = 12) (Fig. 5*C*). Similarly, the I_P-V curve at 60 mM gua^+_o (gray stars, n = 11) falls to the left, whereas the curve at 120 mM Na^+_o (black squares, n = 21) falls to the right. The voltage-dependent inhibition in 125 mM NMG^+_o (gray triangles, n = 11) is ≈30% at −200 mV. These data are most easily explained by gua^+ transit through the Na^+-exclusive site to inhibit the Na/K pump in a Na^+-like voltage-dependent manner.

Discussion

Deletion of the five C-terminal residues in the pig α1 was shown to induce a 25-fold reduction in Na^+_i affinity determined as ATP-dependent phosphorylation (3). Given that pump phosphorylation is required to produce charge movement, the dependence of total charge on Na^+_i is an electrophysiological report of the same event. We observed a smaller reduction in Na^+_i affinity from the ΔKESYY deletion (≈10-fold, see Fig. 2*G*), which may represent patch-to-patch variability ($K_{0.5}$ values ranged between 0.5–1.2 mM for RD and 7–12 mM for RDΔKESYY). Alternatively, voltage-dependent Na^+_i binding (10) may contribute to the small difference in apparent Na^+_i affinity between our observations and those of Morth et al. (3) [a Boltzmann fit to the Q–Vs at 5 mM Na^+_i gave $V_{1/2} = -22 \pm 2$ mV in RD (n = 5) and $V_{1/2} = -100 \pm 8$ mV in the RDΔKESYY (n = 4)].

Based on models for external ion release/binding through an access channel with a dielectric coefficient of 0.7 (9), a shift of −100 mV in the center of the Q–V curve (Fig. 2*E*) is roughly equivalent to a 16-fold reduction in Na^+_o affinity (≈25 mV per 2-fold reduction (11, 16). Thus, the ΔKESYY deletion appears to induce comparable reductions in Na^+ apparent affinity on both sides of the membrane. The fact that the voltage dependence of the steady-state I_P at high K^+_o in the presence of Na^+_o was not affected by the deletion (Fig. 3*C*, circles) is consistent with a model of strict sequential external Na^+ release, where exit from the Na^+-exclusive site precedes release from the shared

sites (Fig. 1). Accordingly, if ΔKESYY only reduces Na^+ affinity at the shared sites and does not alter the affinity at the exclusive site (see Fig. S4 and *SI Appendix* for quantitative steady-state predictions of the model), our observations can be explained as follows: (*i*) The I_P–V curve (Fig. 3*C*, circles) is not affected because at near-saturating $[K_o^+]$ [conditions favoring the forward reaction $2K + E2P \rightarrow E2(K_2)$ over the backward $2Na + E2P \rightarrow E2P(Na_2)$ even in nontruncated pumps] the ion binding sites are rapidly occupied by K^+ after Na_o^+ release and a reduction in Na^+ affinity for the shared sites is negligible. (*ii*) Likewise, in the presence of Na_o^+, the reduced $K_{0.5}$ for K_o^+-activation of outward current (Fig. 3*B*, squares) is expected because of reduced competition by Na_o^+ for the shared sites (apparent only at low $[K_o^+]$). (*iii*) Contrary to observations at near-saturating K_o^+, transient current measured at zero K_o^+ involves Na_o^+ rebinding to the shared sites, a phenomenon known to be mildly voltage-dependent (10, 11) [i.e., the backward reaction $2Na + E2P \rightarrow E2P(Na_2)$ precedes the voltage dependent $E2P(Na_2) + Na \rightarrow E2P(Na_3)$]. Thus, the binding and partial occlusion of 2 Na^+ ions to the shared sites must occur before rebinding the third Na^+ to the exclusive site inducing a large displacement of the Q–V curve to more negative potentials (Fig. 2E).

The fact that the maximal outward pump current induced by K^+ (I_{max}, Fig. 3*C*) in normal RD-pumps is inhibited by negative voltages in the presence of external Na^+ indicates that release of Na^+ from the Na^+-exclusive site occurs before the release from the shared sites in the forward direction of the cycle. Thus, voltage-dependent inhibition at saturating K_o^+ arises from rebinding of Na^+ to the exclusive site before release of the second and third Na^+ ions from the shared sites. Given this, together with the lack of effect of the ΔKESYY deletion mutant in the presence of near-saturating K_o^+, combined with the clear effects of the deletion in the absence of K_o^+, our data provide further support for the sequential Na^+ ion release model previously proposed based on fluorescence measurements in membrane preparations (10) and fast voltage clamp measurements (11, 15) and propose the structural correlation that the first Na^+ ion released is from the Na^+-exclusive site. A similar sequence in which the Na^+-exclusive binding site is the last-to-bind to intracellular sites has been proposed by Schneeberger and Apell (17). Thus, it seems that there is a ″last on, first off″ requirement for Na^+ binding and release from the exclusive site from the inside to the outside, respectively. As a corollary, our results illustrate a method to distinguish between mutational effects on the affinities at different ion binding sites by comparing the voltage dependencies of I_P (measured as ouabain-sensitive current at high K_o^+) and transient charge movement (Fig. S4 and *SI Appendix*).

It is important to note that several mutations in this C-terminal region of the Na/K-ATPase α2 subunit have been linked to familial hemiplegic migraine (for review, see refs. 26 and 27). Defects in Na^+ handling like those reported here may lead to a reduced electrochemical Na^+ gradient and could account for etiology of these inherited syndromes. Consistent with this idea, TEVC studies in one such mutant (28), X1021R, a missense mutation that extends the C-terminal domain, indicate a similar reduction in Na_o^+ affinity for external sites. On the other hand, the high-resolution structure of the Na/K pump reveals that the α-subunit's C-terminal domain forms many hydrogen bonds with other internal parts of the protein (3). In particular, the last two Tyr residues (Y1015 and Y1016, pig α1 numbering) appear to interact with charged residues (K766 at the end of TM5 and R933 at the end of TM8), which are conserved in the α subunits of other members of the P-type 2C subfamily (e.g., gastric and nongastric H/K-ATPases). Thus the effects induced by the C-terminal deletion described here may also have underlying clinical relevance for the Na/K pump and may extend to other related ATPases.

Along with a reduced Na^+ affinity for the shared sites, the ΔKESYY deletion appears to allow the downhill flow of Na^+ ions at low $[K_o^+]$. This Na^+-leak is concomitantly linked to the disappearance of a H^+-leak observed in control pumps in the absence of both Na_o^+ and K_o^+ (Fig. S2). It has been proposed that an increase in $[H_o^+]$ makes the internal gate permissive to H^+ and Na^+ (at low Na_o^+) flow through the exclusive Na^+ site (21). Thus, one interpretation of our results may be that the C-terminal deletion alters the intracellular gate and thus destabilizes ion occlusion. Alternatively, disturbing the interactions at the cytoplasmic end of TM5 and TM8, the C-terminal deletion may induce a long-range structural change transmitted to the shared sites formed by residues in TM4, TM5, TM6, and TM8 (5), reducing Na^+ affinity on both sides of the membrane and giving rise to a cation-leak through the exclusive site. The change in selectivity of the inward current from H^+ in normal pumps to Na^+ in truncated pumps is consistent with such a perturbation. However, evaluation of this possibility will require future examination of ion-binding site mutants with reported reduced Na_o^+ affinity (29).

Whether downhill ion flow occurs through a channel simultaneously open to both sides of the membrane is not clear. (Our attempts to study this conductance in patches were hindered by deterioration of the patch-membrane seal following very negative voltage pulses and by the lack of specific reversible cytoplasmic inhibitors.) If so, the open probability and/or the single channel conductance must be very small in Na^+ solutions as Na^+-leak currents in RDΔKESYY pumps at −180 mV are only ≈3-times larger than normal Na/K pumping rates (Fig. 3*C*, open triangles at −180 mV with open circles at 0 mV).

An important result is that the organic cation guanidinium$^+$ appears not only to traverse both truncated and nontruncated pumps, but also to provoke Na^+-like voltage-dependent inhibition of I_P at high K_o^+, in a manner that differs from the voltage-dependent K^+-competitive inhibition by some quaternary amines (30). These findings are most easily explained by gua$^+$ transiting the pathway through the exclusive Na^+ site as proposed by Li et al. (21). This novel effect of gua$^+$ (mean geometric diameter, 4.4 Å) (31) sets minimal dimensions to the access channel normally transited by the first Na^+ ion released from the exclusive site, indicating that Na^+ may move in a hydrated form similar to proposals for Na^+ permeation through VNaC (25). Although our data suggest that this pathway cannot accommodate NMG^+ (mean diameter 7.3 Å) (32), consistent with the inability of NMG^+ to inhibit the pump in a voltage-dependent manner, we cannot be sure whether this access channel is narrower than the pathway opened by palytoxin on the Na/K-ATPase (33). Palytoxin opens a pathway large enough to accomodate organic cations as large as NMG^+ (although with 50× lower permeability than Na^+) and may represent the exposed pathway for access to and from the shared binding sites (34).

Although they appear to differ in size and selectivity, it is not clear yet whether sequential Na^+ release occurs through a single pathway that widens after release of the first ion, or whether different transmembrane segments are involved in forming two different access channel structures. The short lived transient nature of the structure releasing the first Na^+ ion makes this question challenging to tackle experimentally.

Methods

Oocyte Preparation. Oocytes were enzymatically isolated by incubation for 1 h in Ca^{2+}-free OR2 solution containing (in mM): 82.5 NaCl, 2 KCl, 1 $MgCl_2$, 5 mM Hepes (pH 7.4), and 0.5 mg/ml of collagenase Type IA (Sigma-Aldrich), then injected with an equimolar mixture of α1 (22.5 ng) and Xenopus β3 cRNAs, and kept at 15 °C in OR2 with 1.8 mM $CaCl_2$ for 2–6 days until recording.

Molecular Biology. Deletion of the 5 C-terminal residues (ΔKESYY) was achieved by introducing a STOP in lieu of the last Lys codon of the mutant RD-Xenopus α1 subunit, using the QuikChange site-directed mutagenesis kit (Stratagene). RD indicate the double rat-mimicking substitution Q120R-N131D introduced in our template to confer ouabain resistance. Mutagenesis was confirmed by sequencing, and deletion was corroborated by Western blot analysis (Fig. S1). Complementary RNA was transcribed with the mMessage machine kit (Ambion).

Solutions. The Cl-free standard external solutions (Figs. 2 and 3) contained (in mM): 133 methane sulfonic acid (MS), 10 Hepes, 5 $Ba(OH)_2$, 1 $Mg(OH)_2$, 0.5 $Ca(OH)_2$, and 125 of either NMG^+ or Na^+. Because gua_o^+ was added as a Cl^- salt (guanidine-HCl), for comparison, all other solutions in Figs. 4 and 5 contain Cl^- and were composed of (in mM): 10 Hepes, 5 $BaCl_2$, 1 $MgCl_2$, 0.5 $CaCl_2$, and 120 of either NaCl, guanidine-HCl ,or NMG-Cl (pH 7.6 with NMG). K^+ from a 3M K-MS stock was added to these external solutions. The two basic intracellular (bath) solutions for inside-out patches contained (in mM): 120 Glutamic acid, 1 $MgCl_2$, 10 Hepes, 5 EGTA, and 120 Na^+ or NMG^+ (pH 7.6). Intermediate $[Na_i^+]$ were obtained by mixing Na^+ and NMG^+ solutions. MgATP (4 mM) was added from a 200 mM stock solution (pH 7.4 with NMG) and was present in all experiments presented.

Electrophysiology. TEVC recording was made with an Oocyte Clamp amplifier (OC-725C; Warner Instruments), a Digidata 1440 A/D board, a Minidigi 1A, and pClamp software (Molecular Devices). Signals were filtered at 2 kHz and digitized at 5 kHz. Current and voltage microelectrodes had resistances of 0.5–1.2 MΩ and 1–2 MΩ, respectively, when filled with 3 M KCl. Before recording, oocytes were incubated for 1.5 h in a Na^+-loading solution containing (in mM): 90 Na-sulfamate, 20 Na-Hepes, 20 TEA-Cl, and 0.2 EGTA (pH 7.6) and then transferred to a K^+-free OR2 solution containing 10 μM ouabain, until recording.

Giant patch clamp recordings were made 3–6 days after injection with 20 μm-wide fired-polished pipettes coated with sylgard. The pipette solution was the standard Na_o^+ solution with 1 μM ouabain and 5 mM NaCl added (for electrode reversibility) from a 125 mM NaCl solution. An AxoPatch 200B, Digidata 1322 A/D board, and pClamp 8 software (Molecular Devices) were used for data acquisition at 20 kHz (filter 5 kHz). Patches from noninjected oocytes did not present transient currents (n = 3).

Data Analysis. Q–V curves were fitted with the Boltzmann distribution, $Q = Q_m - Q_{tot}/(1 + e^{V\text{-}V1/2)/k_B})$, where k_B is the slope factor related to the steepness of the curve, and $V_{1/2}$ is the center of the distribution. [Ion] dependence of pump currents and charge movement were fit to the Hill equation, $I = I_{max}[K]^{nH}/(K_{0.5}{}^{nH} + [K^+]^{nH})$ for Fig. 3 and Fig. S2 or $Q_{tot} = Q_{max}[Na^+]^{nH}/(K_{0.5}{}^{nH} + [Na^+]^{nH})$ for Fig. 2*F*.

Note Added in Proof. During revision of this article, a paper describing the effects of ΔKETYY in nonsided membrane preparations was published online (35).

ACKNOWLEDGMENTS. We thank Dominique Gagnon, Mark Milanick, and Olaf Andersen for comments on the manuscript. This work was supported by a start-up grant from Texas Tech University Health Sciences Center (to P.A.) and National Institutes of Health Grant GM-061583 (to C.G.).

1. Post RL, Sen AK, Rosenthal AS (1965) A phosphorylated intermediate in adenosine triphosphate-dependent sodium and potassium transport across kidney membranes. *J Biol Chem* 240:1437–1445.
2. Albers RW (1967) Biochemical aspects of active transport. *Annu Rev Biochem* 36:727–756.
3. Morth JP, et al. (2007) Crystal structure of the sodium-potassium pump. *Nature* 450:1043–1049.
4. Geering K, et al. (2003) FXYD proteins: New tissue- and isoform-specific regulators of Na,K-ATPase. *Ann NY Acad Sci* 986:388–394.
5. Ogawa H, Toyoshima Cn (2002) Homology modeling of the cation binding sites of Na^+K^+-ATPase. *Proc Natl Acad Sci USA* 99:15977–15982.
6. Li C, Capendeguy O, Geering K, Horisberger JD (2005) A third Na^+-binding site in the sodium pump. *Proc Natl Acad Sci USA* 102:12706–12711.
7. Peluffo RD, Berlin JR (1997) Electrogenic K+ transport by the Na(+)-K+ pump in rat cardiac ventricular myocytes. *J Physiol* 501(Pt 1):33–40.
8. Gadsby DC, Rakowski RF, De Weer P (1993) Extracellular access to the Na,K pump: Pathway similar to ion channel. *Science* 260:100–103.
9. Sagar A, Rakowski RF (1994) Access channel model for the voltage dependence of the forward-running Na+/K+ pump. *J Gen Physiol* 103:869–893.
10. Heyse S, Wuddel I, Apell HJ, Sturmer W (1994) Partial reactions of the Na,K-ATPase: Determination of rate constants. *J Gen Physiol* 104:197–240.
11. Holmgren M, et al. (2000) Three distinct and sequential steps in the release of sodium ions by the Na^+/K^+-ATPase. *Nature* 403:898–901.
12. Rakowski RF, Vasilets LA, LaTona J, Schwarz W (1991) A negative slope in the current-voltage relationship of the Na^+/K^+ pump in Xenopus oocytes produced by reduction of external $[K^+]$. *J Membr Biol* 121:177–187.
13. Nakao M, Gadsby DC (1989) [Na] and [K] dependence of the Na/K pump current-voltage relationship in guinea pig ventricular myocytes. *J Gen Physiol* 94:539–565.
14. Nakao M. Gadsby DC (1986) Voltage dependence of Na translocation by the Na/K pump. *Nature* 323:628–630.
15. Hilgemann DW (1994) Channel-like function of the Na,K pump probed at microsecond resolution in giant membrane patches. *Science* 263:1429–1432.
16. Holmgren M, Rakowski RF (2006) Charge translocation by the Na+/K+ pump under Na+/Na+ exchange conditions: Intracellular Na+ dependence. *Biophys J* 90:1607–1616.
17. Schneeberger A, Apell HJ (2001) Ion selectivity of the cytoplasmic binding sites of the Na,K-ATPase: II. Competition of various cations. *J Membr Biol* 179:263–273.
18. Apell HJ, Karlish SJ (2001) Functional properties of Na,K-ATPase, and their structural implications, as detected with biophysical techniques. *J Membr Biol* 180:1–9.
19. Wang X, Horisberger JD (1995) A conformation of Na(+)-K+ pump is permeable to proton. *Am J Physiol* 268:C590–595.
20. Rettinger J (1996) Characteristics of Na+/K(+)-ATPase mediated proton current in Na(+)- and K(+)-free extracellular solutions. Indications for kinetic similarities between H+/K(+)-ATPase and Na+/K(+)-ATPase. *Biochim Biophys Acta* 1282:207–215.
21. Li C, Geering K, Horisberger JD (2006) The third sodium binding site of Na,K-ATPase is functionally linked to acidic pH-activated inward current. *J Membr Biol* 213:1–9.
22. Vasilyev A, Khater K, Rakowski RF (2004) Effect of extracellular pH on presteady-state and steady-state current mediated by the Na+/K+ pump. *J Membr Biol* 198:65–76.
23. Gatto C, et al. (2006) Similarities and differences between organic cation inhibition of the Na,K-ATPase and PMCA. *Biochemistry* 45:13331–13345.
24. Hille B (1971) The permeability of the sodium channel to organic cations in myelinated nerve. *J Gen Physiol* 58:599–619.
25. Kellenberger S, et al. (2001) Permeability properties of ENaC selectivity filter mutants. *J Gen Physiol* 118:679–692.
26. Morth JP, et al. (2009) The structure of the Na+,K+-ATPase and mapping of isoform differences and disease-related mutations. *Philos Trans R Soc Lond Ser B* 364:217–227.
27. Pietrobon D (2007) Familial hemiplegic migraine. *Neurotherapeutics* 4:274–284.
28. Tavraz NN et al. (2008) Diverse functional consequences of mutations in the Na+/K+-ATPase alpha2-subunit causing familial hemiplegic migraine type 2. *J Biol Chem* 283:31097–31106.
29. Koenderink JB, et al. (2003) Electrophysiological analysis of the mutated Na,K-ATPase cation binding pocket. *J Biol Chem* 278:51213–51222.
30. Peluffo RD, Hara Y, Berlin JR (2004) Quaternary organic amines inhibit Na,K pump current in a voltage-dependent manner: Direct evidence of an extracellular access channel in the Na,K-ATPase. *J Gen Physiol* 123:249–263.
31. Nutter TJ, Adams DJ (1995) Monovalent and divalent cation permeability and block of neuronal nicotinic receptor channels in rat parasympathetic ganglia. *J Gen Physiol* 105:701–723.
32. Villarroel A, Burnashev N, Sakmann B (1995) Dimensions of the narrow portion of a recombinant NMDA receptor channel. *Biophys J* 68:866–875.
33. Artigas P, Gadsby DC (2004) Large diameter of palytoxin-induced Na/K pump channels and modulation of palytoxin interaction by Na/K pump ligands. *J Gen Physiol* 123:357–376.
34. Takeuchi A, Reyes N, Artigas P, Gadsby DC (2008) The ion pathway through the opened Na(+),K(+)-ATPase pump. *Nature* 456:413–416.
35. Toustrup-Jensen MS, et al. (2009) The C-terminus of Na^+,K^+-ATPase controls Na^+ affinity on both sides of the membrane through Arg^{935}. *J Biol Chem* 284:18715–18725.